Less Is More? Balancing Identifiability and Predictive Accuracy in Cardiovascular Model Reduction

Maarten Volkaerts[1], Ning Wang [2], Giovanni Samaey [1], Xu Xu [2], Richard Clayton [2]

[1] NUMA, Department of Computer Science, KU Leuven, Leuven, Belgium
[2] School of Computer Science, University of Sheffield, Sheffield, United Kingdom

Abstract

To improve the treatment of pulmonary arterial hypertension, personalized cardiovascular models have been proposed. However, detailed cardiovascular models depend on a large number of parameters, which cannot be reliably estimated from routinely available clinical data. Therefore, we construct a reduced-complexity two-ventricle model and investigate whether it improves practical identifiability of its parameters while maintaining predictive dynamics. We show that nine out of thirteen model parameters are influential using global sensitivity analysis and that seven of the influential parameters are identifiable from synthetic clinical indices using profile likelihood analysis. Actual calibration is done using a Bayesian inference framework and a Markov chain Monte Carlo method. When calibrated to data generated by a four-chamber model, our model closely reproduces the overall cardiovascular dynamics. However, it does not fully capture atrial filling effects or ventricular relaxation, and predictions in the venous compartments remain uncertain. These results characterise the trade-off between parameter identifiability and physiological detail and show which dynamics can and cannot be recovered with our model.

1. Introduction

Effective management of pulmonary arterial hypertension (PAH) requires an understanding of disease progression based on infrequently acquired clinical measurements [1]. In this context, patient-specific digital twins could support clinical decision-making by predicting disease trajectories and evaluating therapeutic interventions *in silico* [2].

Accurate calibration of cardiovascular models to clinical data is a key challenge in the development of such twins. Of all 0D lumped-parameter models, four-chamber models offer the highest degree of physiological detail [3]. However, they contain a large number of unknown parameters, which causes identifiability issues. Many parameters are typically fixed to values reported in the literature, which may introduce modelling bias [4].

In our work, we investigate whether model complexity reduction resolves the identifiability issues and how this impacts modelling accuracy. We construct a simplified two-ventricle model for Bayesian calibration to clinical indices and determine the influential and practically identifiable parameters based on global sensitivity analysis (GSA) and profile likelihood (PL) analysis. We first verify parameter recovery using synthetic data generated by the reduced model. Finally, we calibrate to detailed four-chamber model data to evaluate our model's ability to reproduce pressure and volume traces that are not used for calibration. This reveals which dynamics are preserved by our model and which ones are lost.

2. Methodology

2.1. Two-ventricle model

Our two-ventricle model is shown with its electrical circuit representation in Figure 1. The model has six compartments: left and right ventricles (with subscripts lv and rv, respectively), pulmonary arteries (pul) and veins (pvn), systemic arteries (sys) and veins (svn). Each compartment is modelled by the three equations describing pressure (in mmHg), volume (in ml), and outward flow (in ml/s):

$$P_k = \frac{V_k - V_{0,\mathrm{k}}}{C_k} \quad q_k = \frac{P_k - P_{k+1}}{R_{k\to k+1}} \quad \frac{dV_k}{dt} = q_{k-1} - q_k \tag{1}$$

where k, $k-1$ and $k+1$ refer to the current, past and next compartments, respectively. The resistance $R_{k\to k+1}$ refers to the resistance between compartment k and the next, so either $R_{k\to k+1} = R_k$ or $R_{k\to k+1} = R_{\mathrm{valves}}$ (see Figure 1). Finally, the ventricles have time-varying compliances: $C_k(t) = \frac{1}{E_k(t)} = \frac{1}{E_{\min,\mathrm{k}} + (E_{\min,\mathrm{k}} - E_{\min,\mathrm{k}})a(t)}$ with

$$a(t) = \begin{cases} \sin^2\left(\frac{\pi \bmod(t, T_{\mathrm{cycle}})}{0.7\sqrt{T_{\mathrm{cycle}}}}\right), & \frac{\mathrm{mod}(t,T_{\mathrm{cycle}})}{\sqrt{T_{\mathrm{cycle}}}} < 0.7, \\ 0, & \frac{\mathrm{mod}(t,T_{\mathrm{cycle}})}{\sqrt{T_{\mathrm{cycle}}}} \geq 0.7. \end{cases} \tag{2}$$

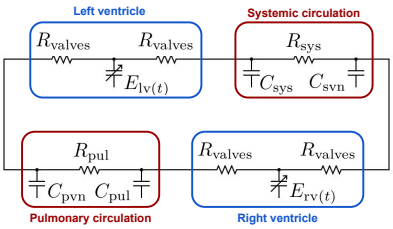

Figure 1. Our model's electrical circuit schematic using resistances (R, in mmHg s/ml), compliances (C, in ml/mmHg), and elastances (E, in mmHg/ml).

The model parameters to be calibrated are grouped in ϑ:

$$\vartheta = [E_{\text{max,lv}}, E_{\text{min,lv}}, E_{\text{max,rv}}, E_{\text{min,rv}}, C_{\text{sys}}, C_{\text{pul}}, R_{\text{pul}}, R_{\text{sys}}, C_{\text{pvn}}, C_{\text{svn}}, R_{\text{valves}}, V_{0,\text{lv}}, V_{0,\text{rv}}, T_{\text{cycle}}]. \quad (3)$$

T_{cycle} can be measured directly and is set to 60 ms for our synthetic data sets. For the other parameters, we determine a biologically plausible range. These ranges, together with all other specifications about our numerical methods and experiments, can be found in the code repository[1].

2.2. Calibration data: clinical indices

As data, we consider a set of clinical indices that are typically available for PAH patients in clinical practice:

$$y = [\text{CO, minPAP, maxPAP, meanPAP, minSAP, maxSAP, meanSAP, ESV}_{\text{lv}}\text{, EDV}_{\text{lv}}\text{, ESV}_{\text{rv}}\text{, EDV}_{\text{rv}}]. \quad (4)$$

Right-heart catheterization offers the cardiac output (CO) and the maximum, mean, and minimum pulmonary arterial pressures (PAP). Routine blood pressure measurements yield the maximum, mean, and minimum systemic arterial pressures (SAP). Finally, cardiac magnetic resonance imaging measures the end-diastolic volumes (EDV) and end-systolic volumes (ESV) of both ventricles.

We perform two calibration experiments using synthetic data. The first dataset $y_{2\text{v}}$ is generated by simulating our two-ventricle model with a prescribed parameter vector, $\vartheta = \vartheta_{\text{true}}$. The second dataset y_{KS} is obtained by simulating a detailed four-chamber Korakianitis-Shi model [3]. For both datasets, we add measurement noise $\eta \sim \mathcal{N}(0, \text{diag}((0.025y_j)^2))$.

2.3. Bayesian inference and MCMC

The data y do not match the model output $\mathcal{F}(\vartheta)$ exactly due to measurement errors η:

$$y = \mathcal{F}(\vartheta) + \eta. \quad (5)$$

[1]The GitLab repository will be made public for the final submission

We formulate the parameter estimation as a Bayesian inference problem and target the posterior distribution

$$P(\vartheta|y) = \frac{L(y|\vartheta)P(\vartheta)}{P(y)}. \quad (6)$$

For the prior distribution $P(\vartheta)$, we consider a uniform distribution over the biologically plausible range of each parameter. The likelihood $L(y|\vartheta)$ quantifies how likely data ϑ resulted in the data y prediction based on the assumed measurement-error model. Finally, $P(y)$ denotes the evidence and acts as a normalization constant.

The posterior distribution yields parameter estimates through its mean, $\bar{\vartheta} = \mathbb{E}_{P(\vartheta|y)}[\vartheta]$, and quantifies the uncertainty associated with these estimates through the posterior variance, $s_\vartheta = \mathbb{E}_{P(\vartheta|y)}[(\vartheta - \bar{\vartheta})^2]$. We estimate the posterior using an MCMC sampling method. We use the adaptive Metropolis algorithm [5] to generate 40 000 posterior samples, of which 20 000 are discarded as burn-in.

2.4. Parameter subset selection

Even for our simplified cardiovascular model, full identifiability of the parameter ϑ from the clinical data y is not guaranteed. Therefore, we employ a parameter subset selection procedure to target the parameters that are both influential for model behaviour and practically identifiable.

The procedure consists of two steps. First, we perform a GSA to rank the parameters according to their influence on the clinical indices. We compute the total Sobol indices $S_T^{i,j}$ to measure the sensitivity of the output y_j to parameter ϑ_i, where the subscripts refer to the corresponding elements in ϑ and y. This total Sobol index is defined as

$$S_T^{i,j} = 1 - \frac{\text{Var}_{\vartheta_{\sim i}}\left(\mathbb{E}[y_j \mid \vartheta_{\sim i}]\right)}{\text{Var}(y_j)} \quad (7)$$

where $\vartheta_{\sim i}$ denotes the ϑ with its i'th element removed. We calculate these indices with Saltelli sampling over the parameter ranges based on 100 000 samples, as implemented in UQLab [6]. We partition ϑ into a set of influential parameters ϑ_A and non-influential parameters ϑ_B.

Next, we assess the identifiability of the influential parameters ϑ_A using PL analysis for $y_{2\text{v}}$. The PL associated with the i-th component of ϑ_A is defined as

$$PL_i(\vartheta_{A,i}) = \min -\log(L(\vartheta_{A,\sim i} \mid \vartheta_{A,i}, y)), \quad (8)$$

where the optimization is performed over $\vartheta_{A,\sim i}$ by performing interior-point optimization from 50 different starting values. In this way, the best achievable likelihood is determined for each fixed value of $\vartheta_{A,i}$.

Then, we derive confidence intervals (CIs) by comparing the PL to the corresponding χ^2-distribution:

$$\text{CI}(\vartheta_{\text{A,i}}) = \left\{\vartheta_{\text{A,i}} \mid 2\left(\text{PL}_\text{i}(\vartheta_{\text{A,i}}) - (-\text{LL}_{\text{MLE}})\right) \leq \Delta(\alpha)\right\} \quad (9)$$

where LL_{MLE} is the maximum log-likelihood value over ϑ_A and $\Delta(\alpha) = icdf(\chi^2_1, 1-\alpha)$. Identifiable parameters are characterized by narrow and finite confidence intervals, whereas unidentifiable parameters exhibit flat PL curves, resulting in wide or unbounded confidence intervals [7].

Based on this analysis, the parameter subset ϑ_A is further divided into two groups: ϑ_{A1}, containing the identifiable parameters, and ϑ_{A2}, containing the unidentifiable parameters. In this work, the parameters in ϑ_{A1} are calibrated, and the others are fixed to their nominal values.

3. Results

3.1. Parameter selection procedure

We start by performing the parameter selection. Figure 2 shows the total Sobol indices $S_T^{i,j}$ for each input-output pair ϑ_i-y_j. Three parameters have low total Sobol indices overall, implying low impact on all outputs: C_{sys}, R_{valves} and $V_{0,\text{lv}}$. Besides these, we also fix $V_{0,\text{rv}}$ as its impact on right ventricular volumes can also be captured by right ventricular elastances. We divide as follows:

$$\vartheta_A = [E_{\text{max,lv}}, E_{\text{min,lv}}, E_{\text{max,rv}}, E_{\text{min,rv}}, C_{\text{pul}}, R_{\text{sys}}, R_{\text{pul}}, C_{\text{svn}}, C_{\text{pvn}}].$$

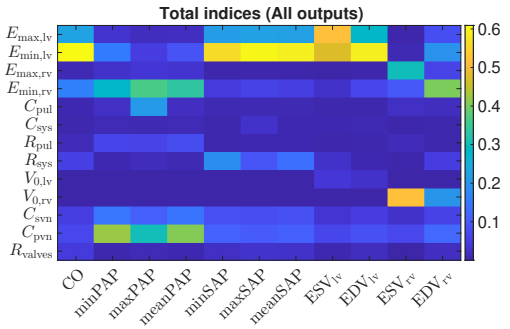

Figure 2. Total Sobol indices $S_{i,j}^T$ for all input-output pairs appearing in ϑ and y.

Figure 3 shows the PL curves based on $y_{2\text{v}}$. Only C_{svn} and C_{pvn} have flat PL curves and CIs wider than their prior range. All other parameters have narrow CIs, implying strong identifiability. This results in the following division:

$$\vartheta_{A1} = [E_{\text{max,lv}}, E_{\text{min,lv}}, E_{\text{max,rv}}, E_{\text{max,rv}}, \quad (10)$$
$$R_{\text{sys}}, C_{\text{pul}}, R_{\text{pul}}]. \quad (11)$$

3.2. MCMC calibration

Figure 4 shows the model calibration to $y_{2\text{v}}$. The top row presents trace plots of the Markov chains generated

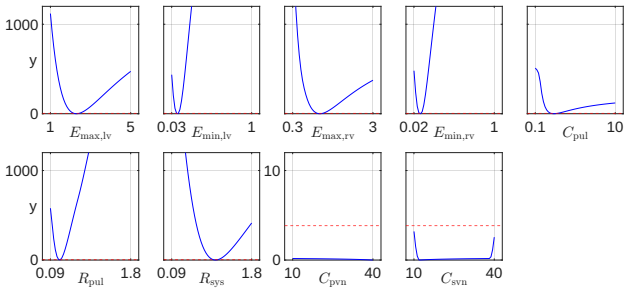

Figure 3. PL study for ϑ_A based on $y_{2\text{v}}$. The CI equals the range where the blue line ($-2\left(PL_i(\theta_{A,i}) - LL_{\text{MLE}}\right)$) lies underneath the red dashed line ($\Delta(0.05)$).

inside the MCMC algorithm. Visual inspection of the trace plots suggests rapid convergence and adequate mixing. The middle and bottom rows display the marginal posterior distributions of the individual parameters. These appear narrowly concentrated around the ground-truth values, indicating that the parameter estimates are accurate and associated with only limited residual uncertainty.

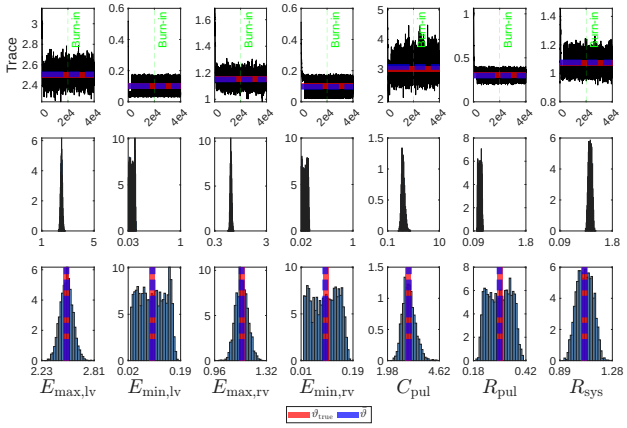

Figure 4. MCMC calibration of for ϑ_{A1} to $y_{2\text{v}}$. Top row: the trace plots of the Markov chain. Middle and bottom row: the marginal posteriors, where the range of the x-axis spans the prior range, or zoomed in on the high-posterior region, respectively.

3.3. Calibrated model evaluation

Finally, we evaluate the accuracy of calibrated model outputs that are not included in the calibration data $y_{2\text{v}}$ and y_{KS}. For the former, Figure 5 shows close visual agreement between the predicted and ground-truth traces after calibration to $y_{2\text{v}}$. This result is expected, as $\bar{\vartheta}$ closely matches ϑ_{true}. Due to the absence of measurements originating from the systemic and pulmonary veins, substantial uncertainty in their predicted pressure is observed. For calibration to y_{KS}, Figure 6 indicates that the reduced model cap-

tures the overall shape of most reference traces. However, we also observe that our model does not capture atrial filling and underestimates the minimum ventricular pressure and the rate of pressure decline during relaxation. While reducing model complexity improves parameter identifiability, it costs physiological detail.

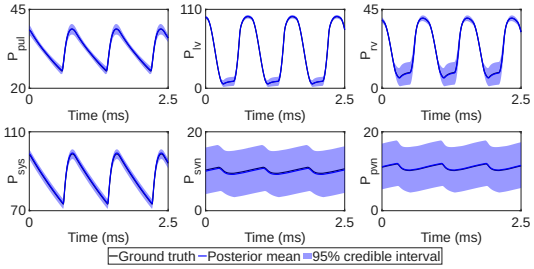

Figure 5. Pressure traces (in mmHg) of ground truth and prediction with credible intervals for calibration to y_{2v}

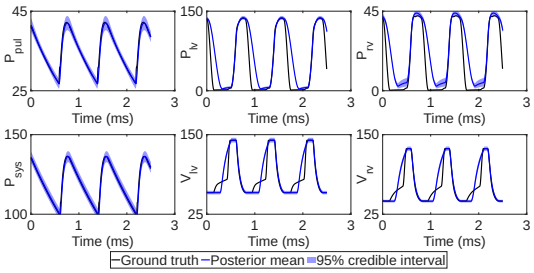

Figure 6. Ventricular pressure (in mmHg) and volume (in mL), and pulmonary and systemic arterial pressures (in mmHg) of ground truth and prediction with credible intervals after calibration to y_{KS}.

4. Conclusion and further work

Our results support the suitability of a two-ventricle cardiovascular model for synthetic calibration tasks. Our analysis based on GSA and PL indicated that seven of the nine influential model parameters are practically identifiable. The MCMC results suggest that their posterior distributions are concentrated around the ground-truth values, with limited residual uncertainty.

The proposed model allows seven of its thirteen parameters to be calibrated, while the remaining parameters are fixed at nominal values. Although the reduction in model complexity inevitably sacrifices physiological detail, our results suggest that the model reproduces the overall shape of the ventricular pressure and volume traces and pulmonary and systemic arterial pressure traces. More highly parameterized models often require many parameters to be fixed independently of the available data during calibration, potentially yielding overconfident predictions in aspects of the system that are only weakly informed by measurements. These results suggest that the reduced model provides a useful balance between identifiability and predictive accuracy. Quantifying this gain relative to calibration of the four-chamber model remains a subject for future work. Furthermore, both models could be used in a complementary manner, combining data-driven parameter estimation with more detailed system representations.

Future work should investigate the trade-off between approximation error and identifiability in greater detail. One possible direction is to quantify how misspecification of fixed parameters affects both parameter estimates and model predictions. In addition, applying the proposed framework to clinical patient data would provide an important assessment of its practical utility.

Acknowledgments

Our work was partially funded by the KU Leuven Research Council through grant IDN/22/006, the Research Foundation – Flanders (FWO) predoctoral grant 1S53625N and travel grant V419626N. N.W., R.C and X.X. are funded by the UKRI EPSRC grant - Networks of Cardiovascular Digital Twins (CVD-Net, EP/Z531297/1).

References

[1] Humbert M, Kovacs G, Hoeper MM, Badagliacca R, Berger RM, Brida M, et al. 2022 esc/ers guidelines for the diagnosis and treatment of pulmonary hypertension. Eur Respir J 2023; 61(1):0–114.

[2] Niederer SA, Balmus M, Burr C, Chico TJA, Clayton RH, Bai W, et al. Digital twins for cardiopulmonary medicine: the case for pulmonary arterial hypertension. Am J Respir Crit Care Med 2026;212(6):1203–1213.

[3] Korakianitis T, Shi Y. Numerical simulation of cardiovascular dynamics with healthy and diseased heart valves. J Biomech 2006;39(11):1964–1982.

[4] Colunga AL, Colebank MJ, REU Program, Olufsen MS. Parameter inference in a computational model of haemodynamics in pulmonary hypertension. J R Soc Interface 2023; 20(200):20220735.

[5] Haario H, Saksman E, Tamminen J. An Adaptive Metropolis Algorithm. Bernoulli 2001;7(2):223–242.

[6] Marelli S, Sudret B. UQLab: A framework for uncertainty quantification in Matlab. ICVRAM 2014;2554–2563.

[7] Colebank MJ. Assessing parameter identifiability of a hemodynamics PDE model using spectral surrogates and dimension reduction. PLoS Comput Biol 2025;21(10):e1013553.

Address for correspondence:

Maarten Volkaerts
Celestijnenlaan 200a, 01.42
maarten.volkaerts@kuleuven.be